ENHANCING THE QUALITY OF HIGHLY HAZED IMAGE USINGCOLOR ATTENUATION PRIORAND FUZZY LOGIC

[1]Deepika Ingle,[2]Yogesh Rathore
[1]M. Tec Student,[2]Asst. Professor
[1]Computer Science and Engineering
[1]Raipur Institute of Technology and Engineering (RITEE), Raipur, Chhattisgarh

Abstract— This paper presents fuzzy logic and color attenuation prior based models for remove haze of an image. By creating a linear model for modelling the scene depth of the hazy image under this novel prior and learning the parameters of the model with a supervised learning method, the depth information can be well recovered. The result of that is used as the input of fuzzy logic. This paper presents the design of the technique using fuzzy inference system for contrast enhancement. The aim is to remove haze from a hazy image and it can be achieving by generate an image of higher contrast than the original image by giving a larger weight to the gray levels that are closer to the mean gray level of the image. This approach is applicable to a dehaze image of all type. Experimental results confirm that our method is very effective for both efficiency and the dehazing effect while preserving the small and sharp details in the image.

***IndexTerms*— Air light, Image Dehazing, Contrast enhancement, Dark channel prior, Fuzzy Logic, transmission.**

I. INTRODUCTION

In this paper we focus on outdoor images taken in bad weather (e.g., foggy or hazy) usually lose contrast and fidelity, resulting from the fact that light is absorbed and scattered by the turbid medium such as particles and water droplets in the atmosphere during the process of propagation. Moreover, most automatic systems, which strongly depend on the definition of the input images, fail to work normally caused by the degraded images. Therefore, image dehazing as a pre-processing restoration step will benefit numerous algorithms that require image/video analysis. Since the density of the haze is different from place to place and it is hard to detect in the haze image, image dehazing is a challenging task. Early researchers use the traditional techniques of image processing to remove the haze from a single (for instance, history, gram-based dehazing methods). However, the dehazing effect is limited, because a single haze image can hardly provide much information. Later, researchers try to improve the dehazing effect with multiple images. In, polarization-based methods are used for dehazing with multiple images which are taken with different degree of polarization. Naresimhanetal. propose haze removal approaches with multiple images of the same scene under different weather conditions. In dehazing is conducted based on the given depth information

(a) (b) (c)

Figure 1 (a) Haze Image (b) intermediated image (c) dehaze image.

An overview of the proposed dehazing method, physical model. Under the assumption that the local contrast of the haze-free image is much higher than that in the hazy image, Tan propose a novel haze removal method by maximizing the local contrast of the image based on Markov Random Field (MRF). Although Tan's approach is able to achieve impressive results, it tends to produce oversaturated images. Fattal propose to remove haze from color image based on Independent Component Analysis (ICA), but the approach is time-consuming and cannot be used for grayscale image dehazing. Furthermore, it has some difficulties to deal with the dense-haze image. Based on a large amount of observations on haze-free images, He et al. find the dark channel prior (DCP) that, in most of the non-sky patches, at least one color channel has some pixels whose intensities are very low and close to zero. With the help of this prior knowledge, they eliminate the distribution of the thickness of haze, and then recover the haze-free image by the atmospheric scattering model. The DCP approach is simple and effective in most cases. However, it cannot well handle the sky images and is computationally intensive. An improved algorithm, guided image filtering, is proposed in to substitute the time-consuming soft matting used in later. Assuming that the depth of the scene is continuous, Tarel et al. introduce a fast dehazing approach based on the median filter. In this paper, we propose a novel color attenuation prior for image dehazing. This simple but powerful prior can help to create a liner model for the scene depth of the hazy image. By learning the parameters of the linear model with a supervised learning method, the bridge between the hazy image and its corresponding depth map is built effectively. With the recovered depth information, we can easily remove the haze from the single hazy image. The efficiency of this dehazing method is dramatically high and the dehazing effect is also superior to that of popular dehazing algorithms. The remainder of this paper is organized as follows: we review the atmospheric scattering model which is widely used

for image dehazing and give a concise analysis on the parameters of this model. We discuss the proposed approach of recovering the scene depth using the color attenuation prior.

The method of image dehazing with the depth information is described. We present and analyse the experimental results. A known problem inherent in investigation and other observation systems is the need to overcome visibility reducing condition such as: humidity, haze, fog, mist, smoke, dust, snow or rain that might be present in the space between the investigation system and the target being observed. The particles or droplets reduces visibility in two ways; the first way is the actual obscuring of what is behind the particles, and the other way is the effect called "light scattering" caused by light reflection in the particles. Both these effects increase with distance, especially when zooming in on a distant object. Even on what appears to be a fine and clear day, there will most certainly be enough haze or fog in the air to reduce contrast significantly. In poor weather conditions dehaze the image is very perilous issue in applications such as aerial photography, image recognition, driving assistance and visual surveillance. So dehazing the image using this method to improve contrasts of the foggy images and restores the visibility of the scene. Haze is spectrally selective: shorter (blue) wavelengths are scattered more, and longer (red/infrared) wavelengths are scattered less. For this reason, many super-telephoto lenses often incorporate yellow filters or coating to enhance image contrast. Also, if using telephoto lenses there is an extra optical problem. Those lenses have a narrow field of view, allowing bright light outside your image area to affect your image with flare, which reduces contrast. Hence removal of fog requires the estimation of air light map or depth map. Image enhancement and image restoration are the two techniques used in the haze removal image fog fades image value. The haze image leads to loss of information instant of using the enhancement techniques. Enhancement is usually used in the following three cases: noise decreases from image, contrast enhancement of the really dull and bright image, and show up the boundaries of the substance in a blurring image. Noise decrease is the Method of reducing noise forms a signal or an image. In general, images occupied with both digital camera and conventional film cameras will choose noise from a multiple of sources. It is main to removed noise for many uses of these images. Contrast enhancement is capturing clear image from side to side intensity.

II. . METHODOLOGY

Flow chart shown below in figure 2 contain different steps which involve for dehaze an image.

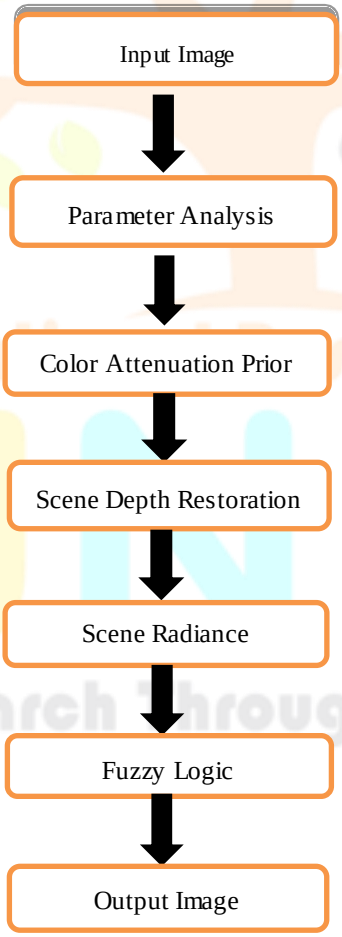

Figure 2 Flow chart of steps involve in dehazing an image

Steps involve in dehazing an image are as follows:

A. INPUT IMAGES

Input images are taken from database of image. Inspired by Tang et al.'s method for preparing the training data, we collect the haze-free images from …http://ivc.uwaterloo.ca/database/Dehaze/Dehaze-Database.php and use them to produce the synthetic depth maps and the corresponding hazy images for obtaining enough training samples. We use this database in your research, and the reference paper listed below:
Kede Ma, Wentao Liu and Zhou Wang, "Perceptual evaluation of single image dehazing algorithms," IEEE International Conference on Image Processing, Sept. 2015 [].

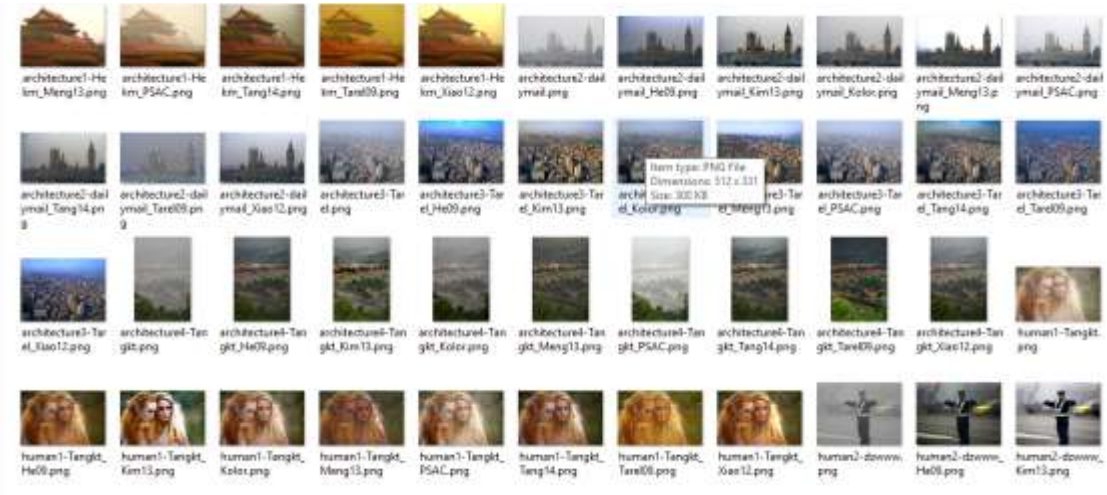

Figure 3 Image database use in our research.

The dataset consists of 25 hazy images covering diverse outdoor scenes and indoor static objects as we see in Figure 3. 22 images of outdoor scenes are captured in the real world and are degraded by haze to different extents, while the hazes of the other 3 indoor images are simulated homogenously. Then 8 dehazing algorithms proposed between 2009 and 2014 are selected to produce 8 different dehazed images for each of the 25 hazy images to form 25 image sets, each of which includes 9 images of the same content (1 hazy, 8 dehazed). In the subjective test, 24 subjects were showed 9 images of one image set at the same time on a display, and were asked to give scores according to perceptual qualities of these images. The score range is from 1 to 10, where 10 indicates the best quality while 1 means the worst. The dataset provided here includes all the 225 images, and all subjective quality scores as well as the Mean Opinion Score (MOS) for each image. Firstly, for each haze-free image, we generate a random depth map with the same size. The values of the pixels within the synthetic depth map are drawn from the standard uniform distribution on the open interval (0, 1). Secondly, we generate the random atmospheric light **A** (k, k, k) where the value of k is between 0.85 and 1.0. Finally, we generate the hazy image **I** with the random depth map d and the random atmospheric light **A** according to Equation (1) and Equation (2). In our case, 500 haze-free images are used for generating the training samples (500 random depth maps and 500 synthetic hazy images).

B. ATMOSPHERIC SCATTERING MODEL

Atmospheric scattering model is widely used for image dehazing and give a concise analysis on the parameter of this model.

$$I(x)=J(x)t(x)+A(1-t(x)) \quad \text{…..(1)}$$

$$t(x)=e^{-\beta}d(x) \quad \text{…..(2)}$$

Here, x= position of pixel within the image, I= Input haze image, J= scene radiance representing haze free image, A=atmospheric light t=medium transmission β=scattering coefficient D =depth of scene. Where,

d = [0, ∞],
I(x)=A and d(x)=∞,
I(x)=A, and d(x)≥d threshold

The pixel belonging to the region with a distant view in the image should have a very large depth d threshold. Assuming every haze image have distinct view.

$$d(x)>=d \text{ threshold}, \; x\epsilon \{x, |\forall y: d(y) \leq d(x)\} \quad \text{……(3)}$$

Based on this assumption, the atmospheric light A is

$$A=I(x), \; x\epsilon \{x, |\forall y: d(y) \leq d(x)\} \quad \text{…..(4)}$$

on this condition the dehazing can be further converted into depth information restoration.

C. COLOR ATTENUATION PRIOR

The brightness and the saturation of pixels in a hazy image vary sharply along with change of the haze concentration. In the haze-free condition, the scene element reflects the energy that is from the illumination source (e.g., direct sunlight, diffuse skylight and light reflected by the ground), and little energy is lost when it reaches the imaging system. The imaging system collects the incoming energy reflected from the scene element and focuses it onto the image plane. Without the influence of the haze, outdoor images are usually with vivid color. In hazy weather, in contrast, the situation becomes more complex. There are two mechanisms in imaging under hazy weather. 1 The direct attenuation cause by reduction in reflected energy lead to low intensity of brightness. 2 The white or gray airlight, which is formed by the scattering of the environment illumination enhances the brightness and reduce the saturation.
Difference between brightness and saturation increase with increase in depth.

$$d(x) \alpha c(x) \alpha v(x) - s(x) \quad \text{….(5)}$$

Where, d= depth, c= concentration of haze, v= brightness and s= saturation.

D. SCENE DEPTH RESTORATION

A. The Linear Model Definition

As the difference between the brightness and the saturation can approximately represent the concentration of the haze, we can create a linear model, i.e., a more accurate expression, as follows:

$$d(x) = \theta_0 + \theta_1 v(x) + \theta_2 s(x) + \varepsilon(x), \quad \text{... (6)}$$

where x is the position within the image, d is the scene depth, v is the brightness component of the hazy image, s is the saturation component,θ_0 ,θ_1 , θ_2 are the unknown linear coefficients, $\varepsilon(x)$ is a random variable representing the random error of the model, and ε can be regarded as a random image. We use a Gaussian density for ε with zero mean and variable σ^2(i.e. $\varepsilon(x) \sim N(0, \sigma^2)$). According to the property of the Gaussian distribution, we have:

$$d(x) \sim p(d(x)|x, ,\theta_0 ,\theta_1 , \theta_2 , \sigma^2) = N(\theta_0 + \theta_1 + \theta_2 s, \sigma^2). \quad \text{.....(7)}$$

One of the most important advantages of this model is that it has the edge-preserving property. To illustrate this, we calculate the gradient of d in Equation (4) and we have:

$$\nabla d = \theta_1 \nabla v + \theta_2 \nabla s + \nabla \varepsilon. \quad \text{....(8)}$$

Due to that σ can never be too large in practice, the value of $\varepsilon(x)$ tends to be very low and close to zero. In this case, the value of $\_\varepsilon$ is low enough to be ignored. A 600×450 random image ε with σ = 0.05 and its corresponding gradient image $\_\varepsilon$ are shown in Figure 4(e) and Figure 4(d), respectively. As can be seen, both the gradient image $\_\varepsilon$ and the random image ε are very dark. It turns out that the edge distribution of d is independent of ε given a small σ. In addition, since v and s are actually the two single-channel images (the value channel and the saturation channel of the HSV color space) into which the hazy image **I** splits, Equation (8) ensures that d has an edge only if **I** has an edge.

(a) (b) (c) (d) (e)

Figure. 4 Illustration of the edge-preserving property of the linear model. (a) The hazy image. (b) The Sobel image of (a). (c) The Sobel image $\nabla d = \nabla v - \nabla s + \nabla \varepsilon$. (d) The Sobel image of (e). (e) The random image ε with σ = 0.05.

We give an example to illustrate this in Figure 4. Figure 4(a) is the hazy image. Figure 4(b) shows the edge distribution of the hazy image. Figure 4(c) shows the Sobel image $\nabla d = \theta_1 \nabla v + \theta_2 \nabla s + \nabla \varepsilon$, where θ_1 is simply set to 1.0, θ_2 is set to −1.0, and ε is a random image as mentioned. As we can see, Figure 4(b) is similar to Figure 4(c) representing that **I** and d have similar edge distributions. This further ensures that the depth information can be well recovered even near the depth discontinuities in the

scene. The linear model works well as we will show later. In the following sections, we use a simple and efficient supervised learning method to determine the coefficients ,θ_0,θ_1, θ_2, and the variable σ2.

B. Learning Strategy

What we are interested in is the joint conditional concentration:

$L = p(d(x1), \ldots, d(xn)|x1, \ldots, xn, ,\theta_0,\theta_1, \theta_2,, \sigma 2),$ ..... (9)

where *n* is the total number of pixels within the training hazy images, *d(xn)* is the depth of the nth scene point, and *L* is the likelihood. Assuming that the random error at each scene point is independent (i.e. $p(\varepsilon 1,\ldots, \varepsilon n) = \_i=1,\ldots,n\ p(\varepsilon i))$, we can rewrite Equation (9) as:

$L=\prod_{1=1}^{n} p(d(xi)|xi,,\theta_0,\theta_1,\theta_2,,\sigma 2)$ .....(10)

According to Equation (5) and Equation (8), we have:

$$L =\prod_{1=1}^{n} \frac{1}{\sqrt{2\pi\sigma^2}} e^{-\frac{dgi-(\theta 0+\theta 1v(xi)+\theta 2s(xi))}{2\sigma 2}},$$ ..... (11)

where *dgi* represents the ground truth depth of the ith scene point. So the problem is to find the optimal values of , θ_0,θ_1, θ_2, and σ to maximum *L*. For convenience, instead of maximizing
the likelihood directly, we maximize the natural logarithm of the likelihood ln *L*. Therefore, the problem can be expressed as follows:

$$\arg\max =\theta_0,\theta_1,\theta_2,\sigma \ln L =\sum_{i=1}^{n} In(\frac{1}{\sqrt{2\pi\sigma^2}} e - \frac{dgi-(\theta 0+\theta 1v(xi)+\theta 2s(xi))}{2\sigma^2}).$$ ....(12)

To solve the problem, we first calculate the partial derivative
of ln *L* with respect to σ and make it equal to zero:

$$\frac{\partial \ln L}{\partial \sigma} = -\frac{n}{\sigma} + \frac{1}{\sigma^3}\sum_{i=1}^{n}(dgi - (\theta 0 + \theta 1v(xi) + \theta 2s(xi)))= 0.$$ ..... (13)

According to Equation (11), the maximum likelihood estimate
for the variable σ2 is:

$$\sigma 2 =\frac{1}{n}\sum_{i=1}^{n}(dgi - (\theta 0 + \theta 1v(xi) + \theta 2s(xi)))2.$$ .....(14)

As for the linear coefficients ,θ_0,θ_1, *and* θ_2, we use the gradient descent algorithm to estimate their values. By taking the partial derivatives of ln *L* with respect to ,θ_0,θ_1, θ_2, respectively,

Algorithm 1. Parameters estimation

Input: the training brightness vector v, the training saturation vector s, the training depth vector d, and the number of iterations t
Output: linear coefficients ,θ_0,θ_1, *and* θ_2, the variable σ^2
Auxiliary functions:
Function for obtaining the size of the vector: n =size(in)
Function for calculating the square: out = square(in)

Begin

1. n = size(v);
2. θ_0 = 0; θ_1 = 1 and θ_2 = -1;
3. sum = 0; wSum = 0; vSum = 0; sSum = 0;
4. **for** iteration from 1to t **do**
5. **for** index from 1 to n **do**
6. temp = d[i] - θ_0 - θ_1 * v[i] - θ_2 * s[i];
7. wSum = wSum + temp;
8. vSum = vSum + v[i] * temp;
9. sSum = sSum + s[i] * temp;
10. Sum = sum + square(temp);
11. **End for**
12. σ^2 = sum/n;
13. θ_0 = θ_0 + wSum; θ_1 = θ_1 + vSum; θ_2 = θ_2 + sSum;
14. **end for**

End

we can obtain the following expressions:

$$\frac{\partial \ln L}{\partial \theta 0} = \frac{1}{\sigma^2}\sum_{i=1}^{n}(dgi - (\theta_0 + \theta_1 v(xi) + \theta_2 s(xi))). \quad \ldots(15)$$

$$\frac{\partial \ln L}{\partial \theta 1} = \frac{1}{\sigma^2}\sum_{i=1}^{n} v(xi)(dgi - (\theta_0 + \theta_1 v(xi) + \theta_2 s(xi))). \ldots(16)$$

$$\frac{\partial \ln L}{\partial \theta 2} = \frac{1}{\sigma^2}\sum_{i=1}^{n} s(xi)(dgi - (\theta_0 + \theta_1 v(xi) + \theta_2 s(xi))). \ldots(17)$$

The expression for updating the linear coefficients can be concisely expressed by:

$$\theta i := \theta i + \frac{\partial lnL}{\partial \theta i} s.t.\ i \in \{0, 1, 2\}. \qquad \ldots(18)$$

It is worth noting that the expression above is used for iterating dynamically, and the notation: = does not express the mathematical equality, but means that setting the value of θi in the left term to be the value of the right term. The procedure for learning the linear coefficients θ_0, θ_1, θ_2 and the variable $\sigma 2$ is shown in Algorithm 1. We used 500 training samples containing 120 million scene points to train our linear model. There are 517 epochs in our case, and the best learning result is that θ_0 = 0.121779, θ_1 = 0.959710, θ_2 = −0.780245, σ = 0.041337. Once the values of the coefficients have been determined, they can be used for any single hazy image. These parameters will be used for restoring the scene depths of the hazy images in this paper.

C. Estimation of the Depth Information

As the relationship among the scene depth *d*, the brightness *v* and the saturation *s* has been established and the coefficients have been estimated, we can restore the depth map of a given input hazy image according to Equation (6). However, this model may fail to work in some particular situations. For instance, the white objects in an image are usually with high values of the brightness and low values of the saturation. Therefore, the proposed model tends to consider the scene objects with white colour as being distant. Unfortunately, this misclassification will result in inaccurate estimation of the depth in some cases. The white geese in the image are the regions for which the model can hardly handle, and these regions are wrongly estimated with high depth values in the depth map. To overcome this problem, we need to consider each pixel in the neighborhood. Based on the assumption that the scene depth is locally constant, we process the raw depth map by:

$$dr(x) = \min_{y \in \Omega r(x)} d(y), \qquad \ldots(19)$$

where $r(x)$ is an $r \times r$ neighborhood centred at x, and dr is the depth map with scale r. However, it is also obvious that the blocking artefacts appear in the image. To refine the depth map, we use the guided image filtering to smooth the image. As can be seen, the blocking artefacts are suppressed effectively.

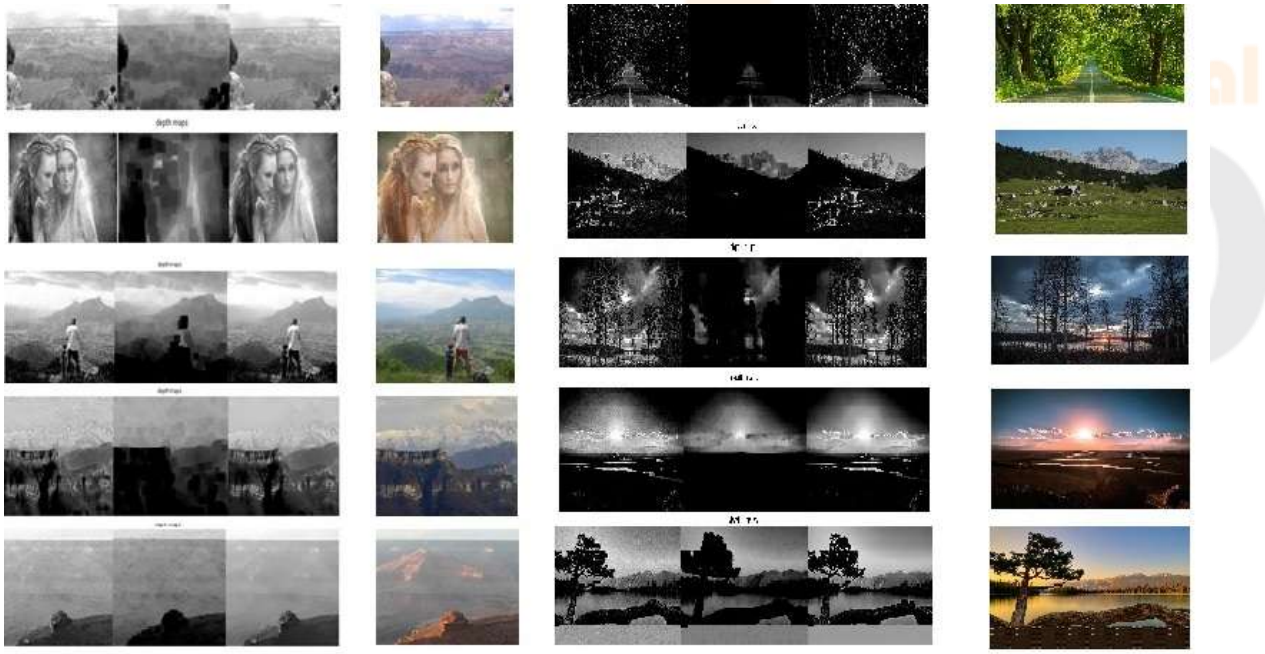

(a) (b) (c) (d)

Figure 5 Example images and the calculated depth maps. (a) The corresponding calculated depth maps (b) Outdoor hazy images (c) calculated depth maps (d) normal image

In order to check the validity of the assumption, we collected a large database of outdoor hazy images from several well-known photo websites (e.g., Google Images) and computed the scene depth map of each hazy image with its brightness and saturation

components according to Equation (6) and Equation (17). Some of the results are shown in Figure 5. Figure 5(b) displays several outdoor hazy images, Figure 5(a) shows the corresponding estimated depth maps. As can be seen, the restored depth maps have darker color in haze-free regions while having lighter colour in dense-haze regions as expected. With the estimated depth map, the task of dehazing is no longer difficult.

E. SCENE RADIANCE RECOVERY

A. Estimation of the Atmospheric Light

We have explained the main idea of estimating the atmospheric light in Section II. In this section, we describe the method in more detail. As the depth map of the input hazy image has been recovered, the distribution of the scene depth is known. Bright regions in the map stand for distant places. According to Equation (4.4), we pick the top 0.1 percent brightest pixels in the depth map, and select the pixel with highest intensity in the corresponding hazy image **I** among these brightest pixels as the atmospheric light **A**.

B. Scene Radiance Recovery

Now that the depth of the scene *d* and the atmospheric light **A** are known, we can estimate the medium transmission *t* easily according to Equation (4) and recover the scene radiance **J** in Equation (3). For convenience, we rewrite Equation (3) as follows:

$$\mathbf{J}(x) = \frac{\mathbf{I}(x) - \mathbf{A}}{t(x)} + \mathrm{A} = \frac{\mathbf{I}(x) - \mathbf{A}}{e^{-\beta d(x)}} + \mathrm{A} \qquad \ldots\ldots(20)$$

For avoiding producing too much noise, we restrict the value of the transmission $t(x)$ between 0.1 and 0.9. So the final function used for restoring the scene radiance **J** in the proposed method
can be expressed by:

$$\mathbf{J}(x) = \frac{\mathbf{I}(x) - \mathbf{A}}{\min\{\max\{e^{-\beta d(x)}, 0.1\}, 0.9\}} + \mathbf{A}, \qquad \ldots\ldots(21)$$

where **J** is the haze-free image we want. Note that the scattering coefficient β, which can be regarded as a constant in homogeneous regions, represents the ability of a unit volume of atmosphere to scatter light in all directions. In other words, β determines the intensity of dehazing indirectly. We illustrate this in Figure 6.

(a) (b) (c) (d) (e) (f) (g)

Figure. 6 Results with a different scattering coefficient β. (a) The hazy image. (b) The final result with $\beta = 0.5$. (c) The final result with $\beta = 0.8$. (d) The final result with $\beta = 1.2$. (e) The restored transmission map with $\beta = 0.5$. (f) The restored transmission map with $\beta = 0.8$. (g) The restored
transmission map with $\beta = 1.2$

Figure 6 (e-g) shows the restored transmission maps with different β, and Figure 6 (b-d) shows the corresponding dehazing results. As can be seen, on the one hand, a small β leads to small transmission, and the corresponding result remains still hazy in the distant regions. On the other hand, a too large β may result in overestimation of the transmission. Therefore, A moderate β is required when dealing with the images with dense-haze regions. In most cases, $\beta = 1.0$ is more than enough.

F. FUZZY LOGIC

Algorithm 2.

1. Convert the image data into fuzzy domain data
2. Membership modification
3. Defuzzification

1. Pseudo code to convert image data into fuzzy domain data:

```
For X=0: M
For Y=0: N
If gray value between zero and min
Then f data=0;
Else if gray value between min and mid
Then f data= (1/ (mid-min) *min+ 1/ (mid-min)) *data;
```

If gray value between mid and max
Then f data = (1 / (max-mid) *mid+ 1/ (max-mid)) *data;
If gray level between max and 255
Then f data=1;

2. Membership Modification:

For X=0: M
For Y=0: N
A) If gray value between zero and min
Then f data=0;
B) If gray value between min and mid
i) If f data between 0 and 0.5
Then f data=2*(f data) ^2
ii) Else if f data between 0.5 and 1
Then f data=1-2*(1-f data) ^2
C) If gray value between mid and max
i) If f data between 0 and 0.5
Then f data=2*(f data) ^2
ii) Else if f data between 0.5 and 1
Then f data=1-2*(1-f data) ^ 2
iii) If gray value between max and 255
Then f data=1

3. Defuzzification:
For X=0: M
For Y=0: N
A) If gray value between zero and min
Then enhanced data=gray value
B) If gray value between min and mid
Then enhanced data= (mid-min)*f data +min
If gray value between mid and max
Then enhanced data= (max-mid)*f data +mid.

G. Parameter Used for The Comparison

We use different parameter for the result comparison, which shows the best result among Qingsong and our method. Time taken to run the method PSNR and MSE are the parameter we used for comparisons.

The mathematical formulae for

1. MSE = $$\frac{1}{MN}\sum_{y=1}^{M}\sum_{x=1}^{N}\left[I(x,y) - I'(x,y)\right]^2$$ …..(22)

2. PSNR = 20 * log10 (255 / sqrt(MSE)). …..(23)

where I(x,y) is the original image, I'(x,y) is the approximated version (which is actually the decompressed image) and M,N are the dimensions of the images. A lower value for MSE means lesser error, and as seen from the inverse relation between the MSE and PSNR, this translates to a high value of PSNR. Logically, a higher value of PSNR is good because it means that the ratio of Signal to Noise is higher. Here, the 'signal' is the original image, and the 'noise' is the error in reconstruction. So, if you find a compression scheme having a lower MSE (and a high PSNR), you can recognize that it is a better one.

III. RESULT ANALYSIS

A. INPUT IMAGE

Input image which are shown below in figure 6 is selected randomly from the database as an input of our method for the comparison with other methods.

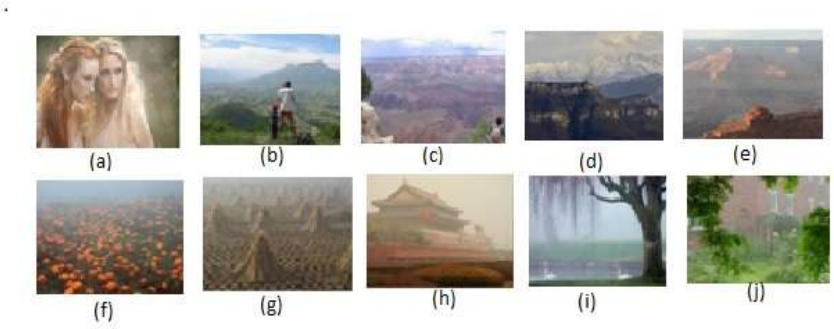

Figure 7. Haze image

The table 1 contain the value of Mean Square Error of dehaze image shown in figure 7 of Qingsong Zhu method and our method. From the table we see that average MSE value of Qingsong Zhu method is 7. 76457e+03 and average MSE of our method is1.63421e+03.

Table 1 Comparison of MSE

Haze image	MSE of dehaze image using Qingsong Zhu method	MSE of dehaze image using our method
a.	7.2678e+03	2.2449e+03
b.	8.5994e+03	1.9138e+03
c.	9.5507e+03	3.1059e+03
d.	5.3969e+03	597.1540
e.	6.8806e+03	2.8671e+03
f.	5.5266e+03	1.1267e+03
g.	4.5206e+03	1.2241e+03
h.	7.6083e+03	892.6541
i.	7.6449e+03	1.4367e+03
j.	4.6499e+03	1.3252e+03
Average	6.76457e+03	1.63421e+03

The graph 8 shows the difference between MSE value of Qingsong Zhu and our method.

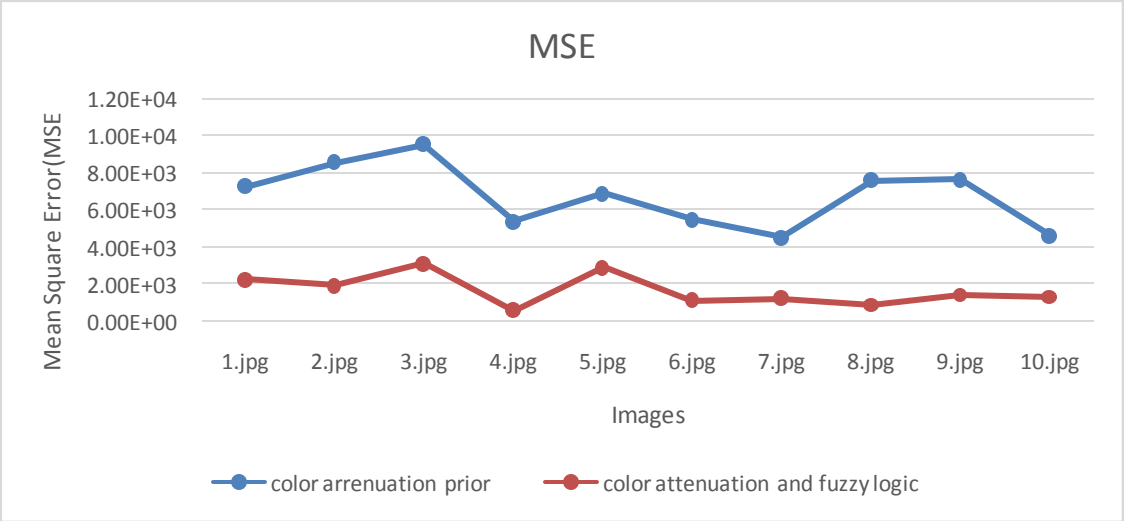

Figure 8. Mean Square Error (MSE) comparison

The table 2 contain the value of Peak signal-to-Noise ratio (PSNR) of dehaze image shown in figure 9 output of Qingsong Zhu method and our method. From the table we see that average PSNR value of Qingsong Zhu method is 10.00549 and average MSE of our method is16.44709.

Table 2 Comparison of PSNR.

Image	PSNR of Qingsong Zhu method	PSNR of our method
a.	9.6426	14.6812
b.	8.8042	15..4803
c.	8.3460	13.2411
d.	10.8095	20.3871
e.	9.7569	13.5577
f.	10.7372	17.6650
g.	11.624	17.3688
h.	9.4195	18.7818
i.	9.3249	16.3519
j.	11.5901	16.9560
Average	10.00549	16.44709

The graph 9. shows the difference between PSNR value of Qingsong Zhu and our method

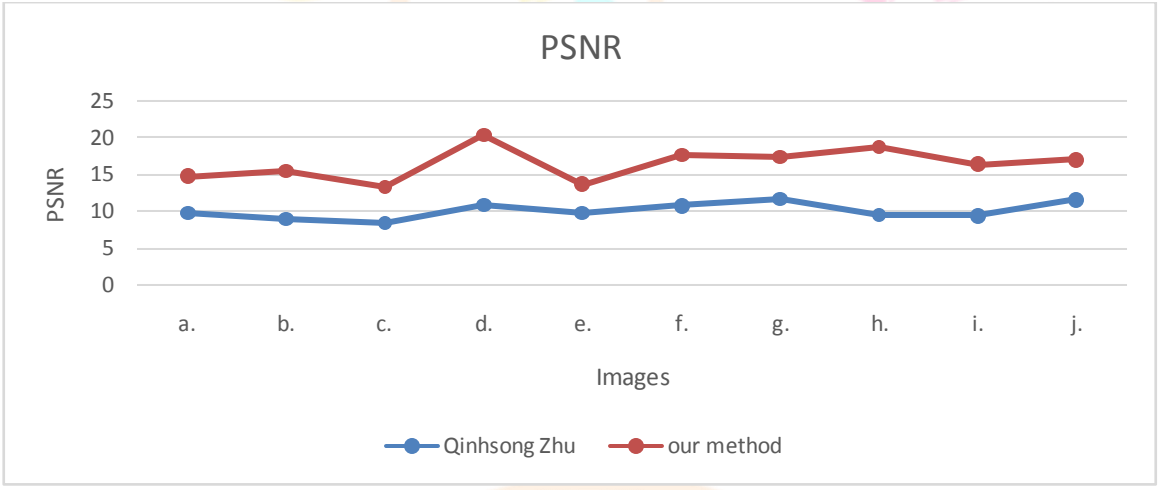

Figure 9. PSNR comparison

The table 2 contain the value of Peak signal-to-Noise ratio (PSNR) of dehaze image shown in figure 1 which is the output of Qingsong Zhu method and our method. From the table we see that average PSNR value of Qingsong Zhu method is 10.00549 and average MSE of our method is16.44709.

Table 3 Total time execution of the method

Images	Qinhsong Zhu Method(second)	Our Method(second)
a.	0.82699	0.795448
b.	0.890812	0.800279
c.	0.734502	0.821726
d.	0.710755	0.788534
e.	1.997243	1.857964
f.	1.080262	0.971615
g.	1.848172	1.335417
h.	0.706451	0.588369
i.	0.840573	0.661547
j.	1.871544	1.359834
Average	1.1507304	0.9980733

The graph 10. shows the difference between time taken by of Qingsong Zhu and our method to execute.

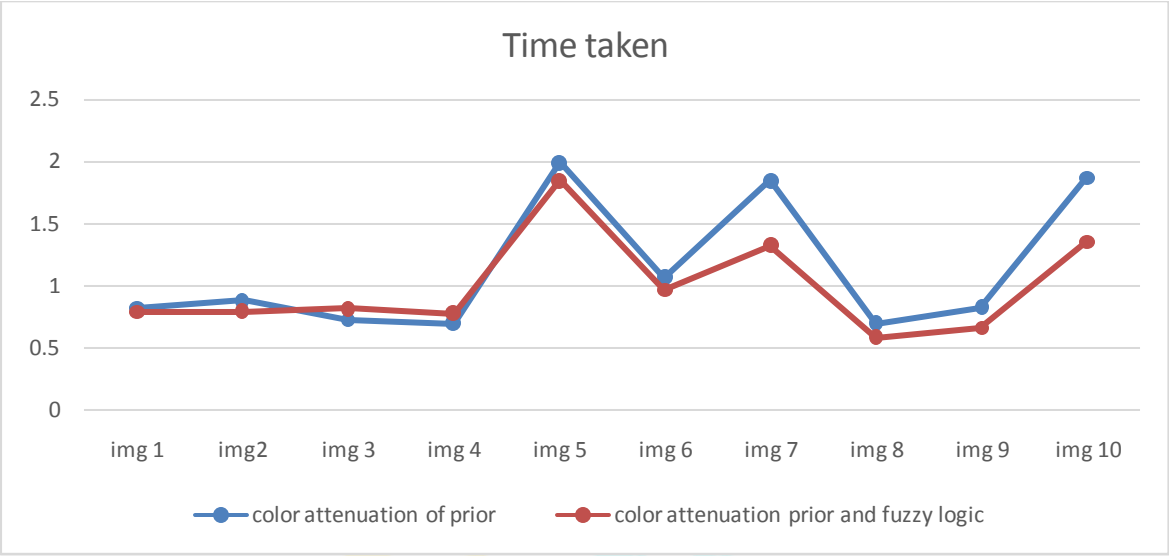

Figure 10. Total execution time of both methods

B. EXPERIMENTAL RESULT

In order to verify the effectiveness of the proposed dehazing method, we test it on various hazy images and compare with Qingsong Zhu method All the algorithms are implemented in the MatlabR2013a environment on a P4-3.3GHz PC with 6GB RAM.

(a) (b) (c)

Figure 11. Qualitative comparison of different methods on real-world images. (a) The hazy images. (b) Qingsong Zhu method. (c) our method

IV. DISCUSSIONSAND CONCLUSSION

We conclude from the figure 10 that total execution time by Qingsong Zhu method is higher than our method. The proposed method is a combination of color attenuation prior algorithm and the fuzzy logic. By creating a linear model for the scene depth of the hazy image with this simple but powerful prior and learning the parameters of the model using a supervised learning method, the depth information can be well recovered. By means of the depth map obtained by the proposed method, the scene radiance of the hazy image can be recovered easily. When we use fuzzy logic it improves the contrast of the image and reduce the haze effect. But due to the contrast improvement in the output dehaze image it increase the darkness which hides some objects present in the image. Experimental results in fig 11. shows that the proposed approach achieves dramatically high efficiency and outstanding dehazing effects as well and also improve the visual appearance of the dehaze image. We further show the MSEs of the results produced by different algorithms in Figure 8. As can be seen, Qingsong Zhu results produce the highest MSEs overall. The high MSEs are mainly because of the over-enhancement as mentioned earlier. Tarel et al.'s results outperform. In contrast, our method achieves the lowest MSEs in from table 1. where Mean Square Error of Qingsong Zhu is compare with our method. From table 2 we conclude that PSNR peak signal noise ratio of Qingsong Zhu is lower than our method. We further show the MSEs of the results produced by Qingsong Zhu method and our method in Figure 8. As can be seen, Qingsong Zhu results produce the highest MSEs overall. The high MSEs are mainly because of the over-enhancement. The average MSE of Qingsong Zhu results is 6.76457e+03, which is more than our method which results is 1.63421e+03. In contrast, our method achieves the lowest MSEs. We further show the PSNRs of the results produced by Qingsong Zhu method and our method in Figure 9. As can be seen, Qingsong Zhu results produce the lowest PSNRs. The average PSNRs of Qingsong Zhu is 10.00549, which is less than our method which results is 16.44709. This shows that our resultant dehaze image quality is higher than Qingsong Zhu resultant dehaze image. Experimental results show that the proposed approach achieves dramatically high efficiency and outstanding dehazing effects as well.

Although we have found a way to model the scene depth with the brightness and the saturation of the hazy image, there is still a common problem to be solved. When we use fuzzy logic it improves the contrast of the image and reduce the haze effect. But due to the contrast improvement in the output dehaze image it increase the darkness which hides some objects present in the image. To overcome this challenge, some more advanced physical models can be taken into account. We leave this problem for our future research.

REFERENCES

1. A Fast Single Image Haze Removal Algorithm Using Color Attenuation Prior, by Qingsong Zhu, Jiaming Mai and Ling Shao, in **IEEE TIP** 2015.
2. R. T. Tan, "Visibility in bad weather from a single image," in *Proc.IEEE Conf. Comput. Vis. Pattern Recognit. (CVPR)*, pp. 1–8
3. Fattal, "Single image dehazing," *ACM Trans. Graph.*, vol. 27, no. 3, p. 72, Aug. 2008.
4. K. He, J. Sun, and X. Tang, "Single image haze removal using dark channel prior," *IEEE Trans. Pattern Anal. Mach. Intell.*, vol. 33, no. 12, pp. 2341–2353, Dec. 2011.
5. J.-P. Tarel and N. Hautiere, "Fast visibility restoration from a single color or gray level image," in *Proc. IEEE 12th Int. Conf. Comput. Vis. (ICCV)*, Sep./Oct. 2009, pp. 2201–2208.
6. Y. Y. Schechner, S. G. Narasimhan, and S. K. Nayar, "Instant dehazing of images using polarization," in *Proc. IEEE Conf. Comput. Vis. PatternRecognit. (CVPR)*, 2001, pp. I-325–I-332.
7. S. Shwartz, E. Namer, and Y. Y. Schechner, "Blind haze separation," in *Proc. IEEE Conf. Comput. Vis. Pattern Recognit. (CVPR)*, vol. 2. 2006, pp. 1984–1991.
8. K. B. Gibson, D. T. Vo, and T. Q. Nguyen, "An investigation of dehazing effects on image and video coding," IEEE Trans. Image Process., vol. 12, no. 2, pp. 662–673, Feb.
9. Shuai Yang, Qingsong Zhu, Jianjun Wang, Di Wu, and Yaoqin Xie "*An Improved Single Image Haze Removal Algorithm Basedon Dark Channel Prior and Histogram Specification"*
10. Weighted Guided image filtering Zhengguo Li, Senior Member, IEEE, Jinghong Zheng, Member, IEEE, Zijian Zhu, Member, IEEE, Wei Yao, member, IEEE and Shiqian Wu, *Senior Member, IEEE*.
11. K. He, J. Sun, and X. Tang, "Guided image filtering," IEEE Trans. Pattern Anal. Mach. Intell., vol. 35, no. 6, pp. 1397–1409, Jun. 2013.
12. Han et al., "Representing and retrieving video shots in human-centric brain imaging space," IEEE Trans. Image Process., vol. 22, no. 7, pp. 2723–2736, Jul. 2013.

13. D. Tao, X. Tang, X. Li, and X. Wu, "Asymmetric bagging and random subspace for support vector machines-based relevance feedback in image retrieval," IEEE Trans. Pattern Anal. Mach. Intell., vol. 28, no. 7, pp. 1088–1099, Jul. 2006.
14. G. Cheng et al., "Object detection in remote sensing imagery using a discriminatively trained mixture model," ISPRS J. Photogramm. Remote Sens., vol. 85, pp. 32–43, Nov. 2013.
15. J. Han, K. Ngan, M. Li, and H.-J. Zhang, "A memory learning framework for effective image retrieval," IEEE Trans. Image Process., vol. 14, no. 4, pp. 511–524, Apr. 2005.
16. J. Han et al., "Efficient, simultaneous detection of multi-class geospatial targets based on visual saliency modeling and discriminative learning of sparse coding," ISPRS J. Photogramm. Remote Sens., vol. 89, pp. 37–48, Mar. 2014.
17. J. Han, D. Zhang, G. Cheng, L. Guo, and J. Ren, "Object detection in optical remote sensing images based on weakly supervised learning and high-level feature learning," IEEE Trans. Geosci. Remote Sens., vol. 53, no. 6, pp. 3325–3337, Jun. 2015.
18. Q. Yang, K.-H. Tan, and N. Ahuja, "Real-time O(1) bilateral filtering," in Proc. IEEE Conf. Comput. Vis. Pattern Recognit. (CVPR), Jun. 2009, pp. 557–564.
19. C. Tomasi and R. Manduchi, "Bilateral filtering for gray and color images," in Proc. 6th Int. Conf. Comput. Vis. (ICCV), Jan. 1998, pp. 839–846.
20. S.G. Narasimhan and S.K. Nayar, "Contrast Restoration of Weather Degraded Images," IEEE Trans. Pattern Analysis and Machine Intelligence, vol. 25, no. 6 pp. 713-724, June 2003.
21. I. Omer and M. Werman, "Color Lines: Image Specific Color Representation," Proc. IEEE Conf. Computer Vision and Pattern Recognition, vol. 2, pp. 946-953, June 2004.
22. M. van Herk, "A Fast Algorithm for Local Minimum and Maximum Filters on Rectangular and Octagonal Kernels," Pattern Recognition Letters, vol. 13, pp. 517-521, 1992.
23. A Novel Optimal Fuzzy System for Color Image Enhancement Using Bacterial Foraging Madasu Hanmandlu, *Senior Member, IEEE*, Om Prakash Verma, Nukala Krishna Kumar, and Muralidhar Kulkarni IEEE TRANSACTIONS ON INSTRUMENTATION AND MEASUREMENT, VOL. 58, NO. 8, AUGUST 2009 2867.
24. Fuzzy Logic Based Filtering for Image De-noising 2016 IEEE International Conference on. Mozammel Chowdhury, Junbin and Gao Rafiqul Islam
25. Crack Detection in Concrete Surfaces using Image Processing, Fuzzy Logic, and Neural Networks Gajanan K. Choudhary and Sayan Dey 2012 IEEE fifth International Conference on Advanced Computational Intelligence(ICACI) October 18-20, 2012 Nanjing, Jiangsu, China.
26. Image Processing - Enhancement, Filtering and Edge Detection Using the Fuzzy Logic Approach. *Ching-Yu Tyan and Paul P. WangDepartment of Electrical EngineeringDuke University*
27. Edge Detection Technique by Fuzzy Logic and Cellular Learning Automata using Fuzzy Image Processing. Jan. 04 – 06, 2013, Coimbatore, INDIA. Dhiraj Kumar Patel Department of Electronics and Communication Prof. Sagar A, (ICCCI -2013).
28. Digital Fuzzy Random Impulse Noise Reduction for Grayscale Images. L.S Usha Rani G.Jagajothi, P.Thiruvalar Selvan.